Laminar and Columnar Development of Barrel Cortex Relies on Thalamocortical Neurotransmission

Hong Li,[1] Sofia Fertuzinhos,[1] Ethan Mohns,[1] Thomas S. Hnasko,[4,6] Matthijs Verhage,[5] Robert Edwards,[4] Nenad Sestan,[1,3] and Michael C. Crair[1,2,3,*]

[1]Department of Neurobiology
[2]Department of Ophthalmology and Visual Science
[3]Kavli Institute for Neuroscience
Yale University School of Medicine, New Haven, CT 06510, USA
[4]Departments of Neurology and Physiology, University of California at San Francisco, San Francisco, CA 94158, USA
[5]Department of Functional Genomics/Clinical Genetics, Center for Neurogenomics and Cognitive Research (CNCR), Vrije Uiniversiteit (VU) and VU Medical Center, Amsterdam, 1081 HV, the Netherlands
[6]Present address: Department of Neurosciences, University of California at San Diego, La Jolla, CA 92093, USA
*Correspondence: michael.crair@yale.edu
http://dx.doi.org/10.1016/j.neuron.2013.06.043

SUMMARY

A dynamic interplay between intrinsic regional molecular cues and extrinsic factors from the thalamus shape multiple features of early cortical development. It remains uncertain and controversial, however, whether the initial formation of cortical columns depends on neuronal activity, and there is little evidence that cortical lamination or neuronal differentiation is influenced by extrinsic activity. We examined the role of thalamic-derived factors in cortical development by selectively eliminating glutamatergic synaptic transmission from thalamocortical neurons in mice and found that eliminating thalamocortical neurotransmission prevented the formation of "barrel" columns in somatosensory cortex. Interestingly, based on cytoarchitectonic criteria and genetic markers, blocking thalamocortical neurotransmission also perturbed the development of superficial cortical lamina and the morphologic development of neurons. These experiments demonstrate that barrels and aspects of the layer-dependent pattern of cortical cytoarchitecture, gene expression, and neuronal differentiation depend on thalamocortical neurotransmission, extending the apparent influence of extrinsic, presumably activity-dependent factors, on cortical development.

INTRODUCTION

A central framework for the study of cortical development concerns the relative role of intrinsic and extrinsic factors in shaping cortical development (Grove and Fukuchi-Shimogori, 2003; O'Leary and Sahara, 2008; Rakic et al., 2009; Sur and Rubenstein, 2005). Cortical arealization, lamination, and neuronal differentiation are generally thought to be intrinsic features of the developing cortex governed by genetic factors (Rakic et al.,

2009). For instance, the development of distinct cortical areas is under the control of diffusible morphogens that govern the specification of frontal, parietal, and occipital regions of the elaborating neuroepithelium (O'Leary and Sahara, 2008). Similarly, the familiar six-layered laminar structure of the neocortex forms as a result of the inside-out chronological migration of newly born postmitotic neurons from the proliferative zone to the nascent cortical plate, with different neuronal subtypes in these layers emerging as the consequence of the combinatorial expression of distinct transcription factors during successive rounds of cell division and migration (Molyneaux et al., 2007; Kwan et al., 2012).

In contrast, some cortical features that emerge later in development, such as aspects of thalamocortical and intracortical neuronal connectivity and the distribution and spacing of cortical columns, are markedly shaped by the sensory periphery during critical periods of development, presumably through activity-dependent mechanisms (Hensch, 2004). For instance, whisker removal or monocular deprivation during an early "critical period" shifts the anatomical and functional properties of neurons in the cortex to favor the remaining nondeprived whiskers or eye. It remains uncertain and controversial, however, whether the initial formation of cortical columns representing peripheral whiskers (so-called barrel columns) in the somatosensory cortex, or ocular dominance columns in the visual cortex, are dependent on neuronal activity (Huberman et al., 2008; Li and Crair, 2011), and there is rather limited evidence that migration, lamination, or the molecular and morphologic elaboration of neurons are sensitive to activity (De Marco García et al., 2011) or extrinsic influences from the thalamus (Miyashita-Lin et al., 1999; Zhou et al., 2010; Sato et al., 2012).

We sought to determine the role of extrinsic, thalamic-derived factors on multiple features of cortical development by examining the effect of eliminating glutamatergic neurotransmission from thalamocortical neurons on cortical development. We found that glutamate release from thalamocortical neurons was absolutely essential for cortical barrel column development. Remarkably, the differentiation of neurons and the elaboration of superficial layers in the cortex were also disrupted upon removal of excitatory input from the thalamus. These experiments help

define limits on the role of intrinsic factors in cortical development and establish a role for extrinsic, presumably activity-dependent factors on cortical columnar, laminar, and neuronal morphological development.

RESULTS

Thalamocortical Neurotransmission Is Eliminated in ThVGdKO Mice

To examine the role of thalamocortical neurotransmission in cortical development, we generated mice in which glutamatergic release is disrupted in thalamocortical neurons using a Cre/loxP recombination approach. We focused on vesicular glutamate transporters, of which there are three known genetic forms in mice ($Vglut1$–3). $Vglut3$ is expressed weakly and sporadically in the brain, while $Vglut2$ and $Vglut1$ have strong and largely complementary expression patterns (Fremeau et al., 2004), with $Vglut2$ robustly expressed in the thalamus and $Vglut1$ to a lesser extent. Because $Vglut2$ null mice die at birth (Moechars et al., 2006), we crossed floxed $Vglut2$ mice ($Vglut2^{fl/fl}$; Hnasko et al., 2010) with the $Sert$-Cre driver line (Zhuang et al., 2005) to delete $Vglut2$ from thalamocortical projection neurons. Somewhat to our surprise, thalamocortical neurotransmission in these mice was indistinguishable from that in control mice (Figures 1A–1E). Reasoning that $Vglut1$ may compensate for the absence of $Vglut2$ in thalamic neurons, we generated mice that lacked $Vglut1$ and $Vglut2$ in the thalamus by crossing $Sert$-Cre mice with $Vglut1^{+/-}$;$Vglut2^{fl/fl}$ mice to generate $Vglut1$ and $Vglut2$ double knockout mice ($Sert$-$Cre^{+/-}$;$Vglut1^{-/-}$;$Vglut2^{fl/fl}$, or ThVGdKO). ThVGdKO mice had severely disrupted thalamocortical neurotransmission, whereas all littermate control mice, even those with just a single copy of $Vglut1$ or $Vglut2$, had thalamocortical neurotransmission that was grossly indistinguishable from that in wild-type (WT) mice (Figure 1).

We measured the effect of $Vglut$ deletion on thalamocortical neurotransmission in two ways. First, we used in vitro electrophysiological techniques to examine miniature excitatory postsynaptic current (mini-EPSC) amplitude and frequency in thalamocortical brain slices (Crair and Malenka, 1995) across a range of ages (postnatal days 4–15, P4–P15). Mini-EPSCs were measured using whole-cell patch-clamp recordings from layer 4 (L4) neurons following thalamic stimulation after replacing Ca^{2+} with Sr^{2+} in the extracellular medium to desynchronize neurotransmitter release (Iwasato et al., 2008). In 5 of 11 ThVGdKO mice at P9–P11, we could not evoke a measurable thalamocortical response. In the remaining six ThVGdKO mice at P9–P11 (Figures 1C–1E), evoked mini-EPSC amplitude (3.9 ± 0.18 pA) and frequency (0.28 ± 0.24 Hz) were much smaller in comparison to littermate controls (p < 0.01). Neither single knockout of $Vglut1$ ($Vglut1^{-/-}$;$Vglut2^{fl/-}$; amplitude: 8.44 ± 1.78 pA; frequency: 8.0 ± 1.18 Hz; n = 6) nor thalamic deletion of $Vglut2$ ($Sert$-$Cre^{+/-}$;$Vglut1^{+/-}$;$Vglut2^{fl/fl}$, amplitude: 12.92 ± 0.99 pA; frequency: 10.24 ± 1.51 Hz; n = 5) significantly reduced thalamocortical neurotransmission in comparison to WT mice (amplitude: 11.84 ± 0.84 pA; frequency: 10.47 ± 2.14 Hz; n = 3). We did not detect any thalamocortical synaptic response at P4–P6 in ThVGdKO mice (n = 4) and detected only very weak response in some slices at P13–P15 that was similar in amplitude

and frequency to that observed at P9–P11 and much smaller than that observed in control littermates (p < 0.001; Figures 1F and 1G). These results indicate that $Vglut1$ and $Vglut2$ can both contribute to glutamatergic neurotransmission at thalamocortical synapses, and elimination of both $Vglut1$ and $Vglut2$ in ThVGdKO mice nearly completely abolishes thalamocortical neurotransmission.

We confirmed these results using in vivo electrophysiological techniques in P9–P12 mice (Figures 1H and 1I). Local field potentials (LFPs) recorded with extracellular multisite silicon array electrodes in somatosensory cortex in response to peripheral whisker stimulation typically produce brief multiphasic events that are dominated by an initial negative-going waveform with greatest amplitude in L4 (Quairiaux et al., 2007). Stimulus-triggered waveform averages in control ($Vglut1^{-/-}$;$Vglut2^{fl/-}$) mice showed robust evoked LFPs (Figure 1I, left; maximum negative amplitudes of 207 μV and 209 μV; maxima at 38 ms and 51 ms, respectively, after stimulus onset; waveform widths at half maximum were 23 ms and 31 ms). The same experimental procedure in ThVGdKO mice failed to elicit evoked potentials (n = 4). Indeed, the stimulus-triggered waveform averages revealed no stimulus-related activity in the LFPs at all (Figure 1I, right). Histology confirmed that the recording probes were placed in similar locations within somatosensory cortex in both groups of mice (data not shown). Together, these results indicate that glutamatergic neurotransmission at thalamocortical synapses in ThVGdKO somatosensory cortex was largely, if not completely, abolished.

ThVGdKO Mice Lack Barrels in the Somatosensory Cortex

Barrels in the somatosensory cortex of mice are composed of clusters of thalamocortical axon arbors in L4 surrounded by rings of spiny stellate neuron somata whose dendrites are oriented toward the center of the barrel to synapse with thalamocortical afferents relaying information from a single whisker (Li and Crair, 2011). We used cytochrome oxidase (CO) histochemistry and Nissl staining to examine whether cortical barrel formation was dependent on thalamocortical glutamatergic neurotransmission. In flattened tangential sections through somatosensory cortex, clear CO barrel patterns were present in $Vglut1^{-/-}$,$Vglut2^{fl/-}$ and all other control mice, while a barrel pattern was not detectable in ThVGdKO mice (Figure 2A, top; Figure S1A available online). This suggests that thalamocortical afferents fail to cluster into barrels in ThVGdKO mice. Using Nissl staining in flattened tangential sections through L4 to examine cortical cytoarchitecture, barrels were again absent in ThVGdKO mice, while clear barrels were evident in all control mice (Figure 2A, bottom). Nissl-stained thalamocortical sections from ThVGdKO mice at P7 and P14 were grossly normal, with the obvious exception of L4 in somatosensory cortex of ThVGdKO mice, which lacked barrels (Figures 2B and 2D, arrows in 2D). Thalamocortical axon innervation of the somatosensory cortex was also grossly normal, as revealed by immunolabeling for serotonin transporter (5-HTT) in thalamocortical axons at P6 (Figure 2C) and direct imaging of thalamocortical afferents at P14 following the injection of a floxed-tdTomato viral construct into the thalamus of $Sert$-Cre mice (Figure 2E), again with the obvious
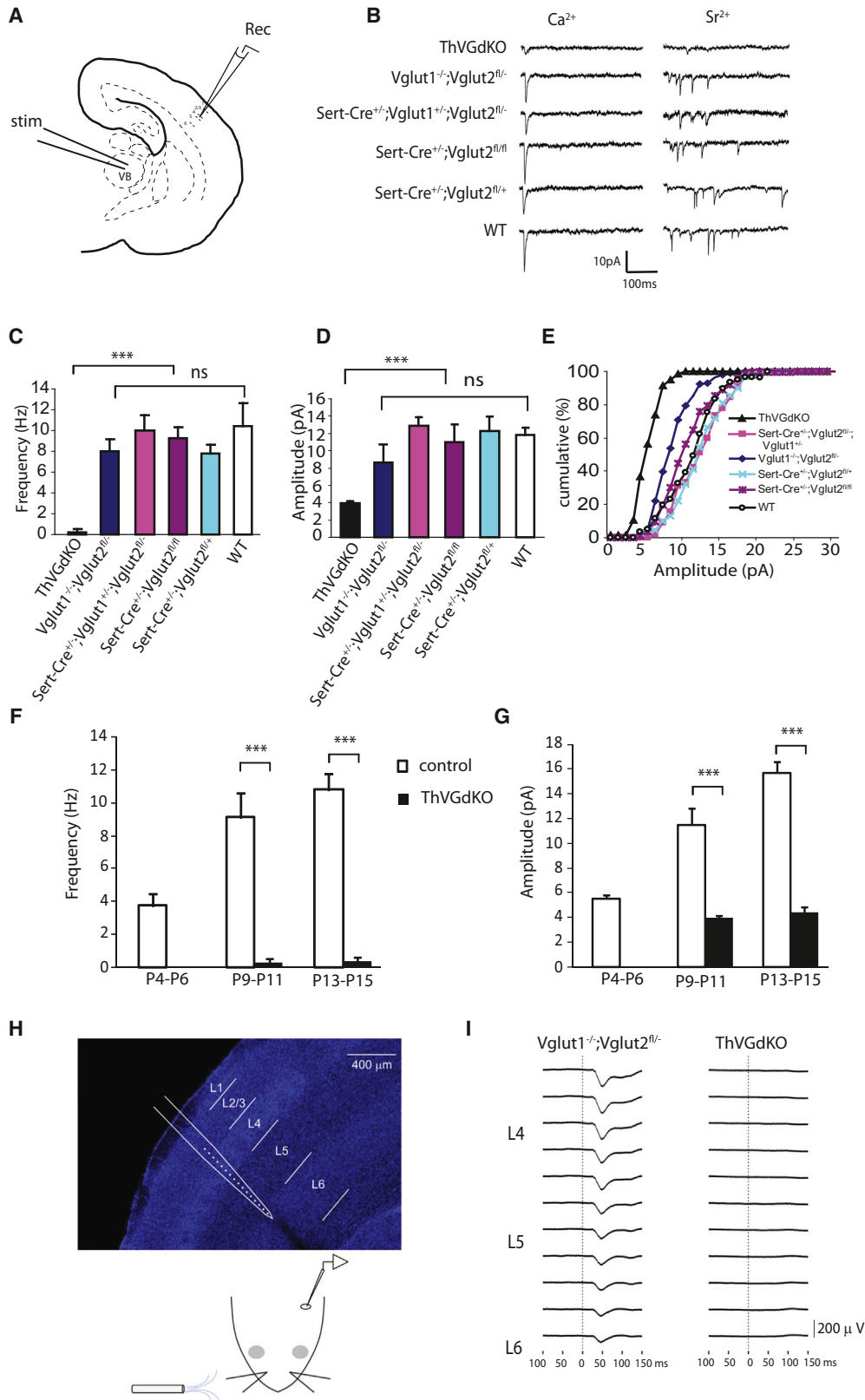
(legend on next page)

exception of disrupted barrel clusters in somatosensory cortex of ThVGdKO mice. The formation of cortical barrels is contingent on intact barrel structures in the thalamus (barreloids) and brainstem (barelettes; Li and Crair, 2011), but CO staining in coronal sections through the ventrobasal thalamus and brainstem showed typical barrel patterns in these structures (Figure S1B). These results indicate that the emergence of cortical cytoarchitecture and the clustering of thalamocortical afferents into a barrel pattern depend critically on glutamatergic neurotransmission in thalamocortical neurons, suggesting a key role for extrinsic, presumably activity-dependent factors in cortical columnar development.

Cortical Lamination Defects in ThVGdKO Mice

The absence of barrels in the somatosensory cortex of ThVGdKO mice is consistent with previous reports showing that cortical barrel topography is sensitively dependent on the presence, number and arrangement of whiskers on the contralateral snout and specifically implicates thalamocortical neurotransmission in communicating the peripheral sensory pattern onto the cortex (Van der Loos and Woolsey, 1973; Welker and Van der Loos, 1986). We wondered whether the elimination of thalamocortical glutamatergic neurotransmission would disrupt cortical laminar organization because the distinctive granular nature of L4 is unique to sensory areas of cortex that receive extensive thalamic innervation. At postnatal day 6 (P6), when barrels have just formed, Nissl staining showed that cortical thickness and lamination in ThVGdKO mice was no different than littermate controls (Figures 2B, 3A, and 3B; Figures S1D and S1E). To our surprise, noticeable differences in cortical lamination emerged in the second week after birth, when superficial layers of the cortex undergo their most dramatic elaboration (Figures 2D, 3C, and 3D; Figure S1F). In particular, the characteristic dense band of granular cells (L4) at midcortical depths was blurred in ThVGdKO mice at P15 and replaced by a relatively cell-sparse layer resembling L5a. These changes were evidenced by a significantly reduced density of cells in ThVGdKO mice at a depth corresponding to L4 in comparison to all littermate control mice (bin 5 in Figure 3D; Figure S1F) and a significantly higher density of cells at a depth corresponding to L5a (bin 6 in Figure 3D). Both at P6 and P15, the total number of Nissl-stained cells (Figure 3E;

P6: control: 438 ± 35, ThVGdKO: 446 ± 26, p = 0.3; P15: control: 378.6 ± 42, ThVGdKO: 365 ± 45, p = 0.15) and caspase-3 positive cells (data not shown) were not different in control and ThVGdKO mice, indicating there was no obvious cell proliferation or apoptosis defects in ThVGdKO mice.

CUX1 (aka CUTL1 or CDP) is a transcription factor expressed in superficial layers of somatosensory cortex that clearly delineates the bottom of L4 (Nieto et al., 2004). As with Nissl staining, there was no difference in the laminar expression of CUX1 at P6 (Figures 3F and 3H). However, there were fewer cells labeled with CUX1 at P15 (Figures 3G, 3I, and 3K), and the thickness of CUX1-expressing superficial layers was significantly reduced in ThVGdKO mice (control: 39% ± 3% of cortical thickness; ThVGdKO: 30% ± 4%; p < 0.01; Figures 3G, 3I, and 3J), consistent with the lamination defects observed with Nissl stain. These results suggest that in the prolonged absence of glutamatergic input from the thalamus, the relative thickness of infragranular layers (L5) of the cortex expands at the expense of granular and supragranular layers (L2/3 and L4) during the second week after birth.

Because *Sert-Cre* is expressed in all the thalamic sensory relay nuclei (Zhuang et al., 2005), including the visual thalamus (dorsal lateral geniculate nucleus or dLGN) and the auditory thalamus (medial geniculate nucleus or MGN), we wondered whether laminar development in visual and auditory cortex was similarly impaired as in the somatosensory cortex. However, we did not observe any obvious cortical laminar cytoarchitecture defects in the visual or auditory cortex of ThVGdKO mice (Figures S2A–S2F). *Sert-Cre* expression is much weaker in the dLGN and MGN in comparison to the somatosensory thalamus (ventrobasal or VB; Figures S3A–S3O), and accordingly *Vglut2* mRNA and VGLUT2 protein levels were only modestly decreased in the dLGN (68.9% of control mRNA levels) and MGN (48.4% of control mRNA levels) of ThVGdKO mice at P12. In contrast, *Vglut2* mRNA in the VB was only 13.5% of control levels (p < 0.001 for the difference between dLGN, MGN, and VB), and VGLUT2 protein levels were down to 20% of control already at P4. This is consistent with the earlier and stronger expression of SERT in the VB relative to the other thalamic relay nuclei (Lebrand et al., 1998) and is probably responsible for sparing the auditory cortex and visual cortex from the laminar

---

Figure 1. Thalamocortical Neurotransmission Is Completely Disrupted in ThVGdKO Mice

(A) Schematic diagram of the in vitro thalamocortical slice used to examine thalamocortical neurotransmission. Stimulating electrode (stim) was placed in the ventrobasal thalamus (VB) and a whole-cell recording electrode (Rec) was placed in L4 of the cortex.

(B) Example of whole-cell recordings from ThVGdKO and littermate controls at P9–P11. To isolate thalamocortical synapse mini-EPSCs, Ca^{2+} (left side) was replaced by Sr^{2+} (right side) in the extracellular medium, which desynchronizes neurotransmitter release.

(C) Evoked mini-EPSC frequency in P9–P11 ThVGdKO and their littermate controls (mean ± SEM). n = 6 for ThVGdKO and n = 3 for each control genotype. ***p < 0.001; ns, nonsignificant.

(D) Quantification of mini-EPSC amplitude in P9–P11 ThVGdKO mice in comparison to littermate controls, ***p < 0.01. Data are presented as mean ± SEM.

(E) Cumulative frequency plot of the amplitude of evoked mini-EPSCs at thalamocortical synapses in P9–P11 ThVGdKO mice and their littermate controls.

(F) Comparison of evoked mini-EPSCs frequency in control and ThVGdKO mice between P4 and P15 (mean ± SEM). No thalamocortical response could be evoked at P4–P6 in ThVGdKO mice, and the frequency of evoked mini-EPSCs remains very low in ThVGdKO in comparison to littermate controls through P15. For ThVGdKO, n = 4 at P4–P6, n = 6 at P9–P11, and n = 3 at P13–P15. For controls, n = 5 at P4–P6, n = 12 at P9–P11, and n = 3 at P13–P15. ***p < 0.001.

(G) Comparison of evoked mini-EPSC amplitude in ThVGdKO and control mice between P4 and P15. In ThVGdKO mice, mini-EPSC amplitudes were much smaller than those in control mice through P15. ***p < 0.001.

(H) Schematic drawing of in vivo local field potential (LFP) recording using a multisite silicon probe in the somatosensory cortex (top panel) while air puffs were delivered to the contralateral snout (bottom panel).

(I) Multiphasic LFP events were recorded during air puff stimulation of contralateral whiskers in *Vglut1*$^{-/-}$;*Vglut2*$^{fl/-}$ and ThVGdKO mice. No stimulated LFP signal was detected in the somatosensory cortex of ThVGdKO mice.
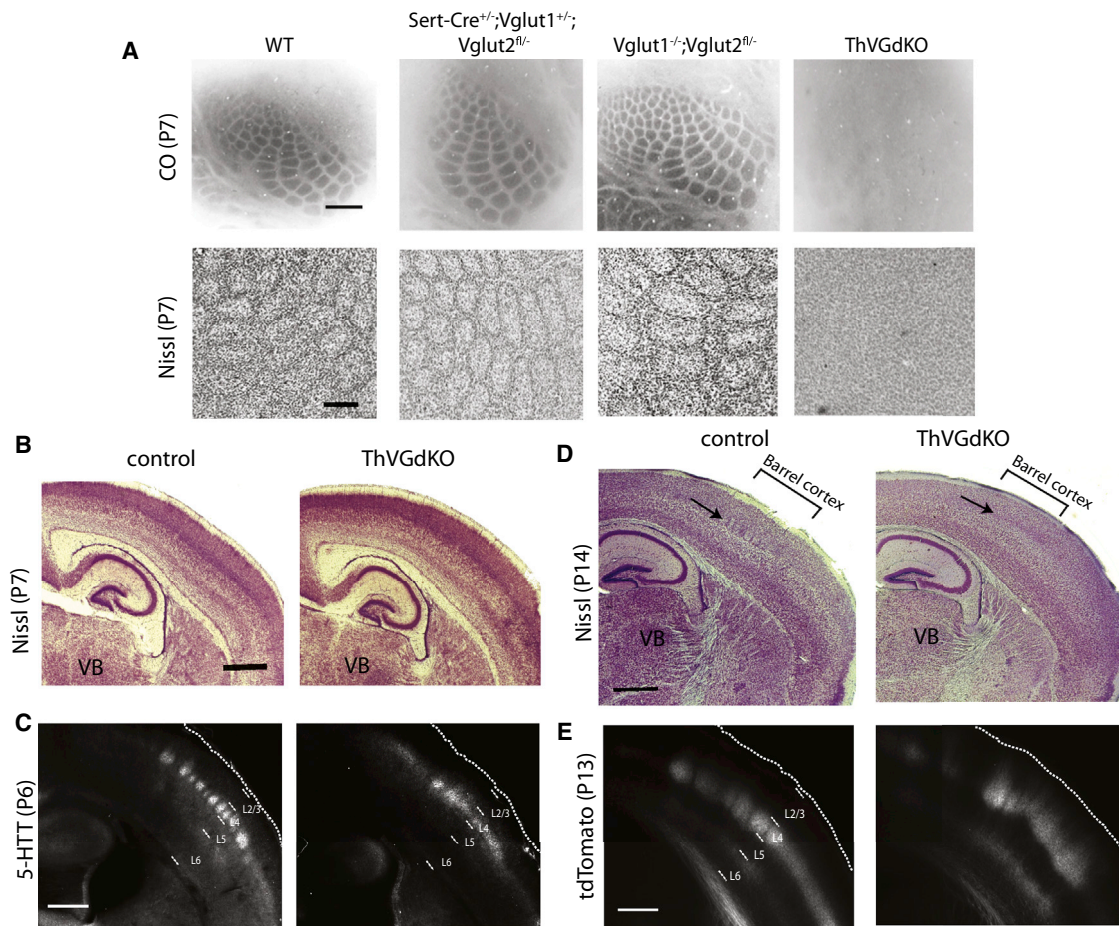
Figure 2. Barrels Are Completely Disrupted in ThVGdKO Mice

(A) Cytochrome oxidase (CO) histochemistry in flattened sections through L4 of ThVGdKO somatosensory cortex and littermate controls (top). Scale bar represents 400 μm. Nissl stain in flattened sections through L4 of ThVGdKO somatosensory cortex and littermate controls (bottom). Scale bar represents 150 μm. Note that barrels are absent in ThVGdKO mice when viewing (presynaptic) thalamocortical afferents (CO) or (postsynaptic) L4 neurons (Nissl).

(B) Low-magnification image of Nissl-stained thalamocortical sections at P7 in control (left) and ThVGdKO mice (right). Cortical lamination appears normal. Scale bar represents 500μm.

(C) 5-HTT immunostaining of thalamocortical axons shows normal innervation of L4 in cortex of ThVGdKO mice at P7 (right), except axons are not clustered into barrels as in control mice (left). Scale bar represents 500 μm.

(D) Low-magnification image of Nissl-stained thalamocortical sections at P15 show no barrels in ThVGdKO mice (arrow on right) and apparently reduced superficial layers (particularly L4) in comparison to control mice (left). Scale bar represents 500 μm.

(E) Thalamocortical axon targeting of cortex, revealed through AAV-tdTomato injection into thalamus, shows grossly normal cortical innervation in ThVGdKO mice (right) at P15 in comparison to control mice (left), although thalamocortical axon clustering into barrels is not apparent, and axon arbors are shifted toward the pial surface in ThVGdKO mice in comparison to control mice. Scale bar represents 500 μm.

See also Figure S1.

changes observed in the somatosensory cortex of ThVGdKO mice.

Lamination Defects Are Not a Necessary Consequence of Barrel Defects

We generated a second model of disrupted neurotransmitter release to confirm and expand our understanding of the role of thalamocortical neurotransmission on somatosensory cortex development. In this case we deleted the gene encoding syntaxin binding protein 1 (*Stxbp1* or *Munc18-1*), which is essential for Ca^{2+}-stimulated neurotransmitter release (Toonen and Ve-

rhage, 2007), from neurons in somatosensory thalamus by crossing *Sert-Cre* mice with floxed *Munc18-1* mice (Dudok et al., 2011) to conditionally delete *Munc18-1* in the thalamus (ThMunc18KO mice). Like ThVGdKO mice, barrels did not form in the somatosensory cortex of ThMunc18KO mice (Figures 4A and 4C), but cortical lamination was normal at P6 (Figures 4C–4E). Moreover, ThMunc18KO mice developed cortical lamination defects at P15 that were similar to those observed in ThVGdKO mice (Figures 4C, 4D, 4F, and 4H), with cell number and cell density significantly reduced in L4, but significantly increased in L5 (Figure 4F). Deletion of *Munc18-1* had a rather

severe effect on thalamic neurons, leading to the death and the eventual degeneration of the somatosensory (VB) thalamus between P0 and P7 (Figure S4), and the absence of cortical innervation by thalamic axons as demonstrated with VGLUT2 immunostaining (Figure 4B). This effect was not observed in ThVGdKO mice (Figures 2B and 2D). Generally, it was difficult to distinguish L4 from L2/3 and L5 in ThMunc18 mice at P15 (Figure 4C), although cortical lamination appeared normal in ThMunc18KO somatosensory cortex at P6 (Figure 4C), as in ThVGdKO mice. The progressive changes in cortical lamination observed in ThVGdKO and ThMunc18KO mice were probably not due to a progressive deletion of *Vglut2* or *Munc18*, because thalamocortical neurotransmission was already absent at P6 in ThVGdKO mice and got no worse thereafter (Figures 1F and 1G), while thalamocortical neuron degeneration in ThMunc18KO mice occurred between P0 and P7 (Figure S4). Thus, thalamocortical innervation had little effect on the initial wave of cortical neuron migration and laminar formation in the first week after birth, although the absence of thalamocortical neurotransmission disrupted barrel formation. We were curious whether the cortical lamination defects observed in ThVGdKO and ThMunc18KO somatosensory cortex were a necessary consequence of abnormal barrel formation, so we also examined cortical laminar development in *barrelless* mice. *Barrelless* is a classic mutant with a spontaneous loss-of-function mutation in adenylate cyclase 1 (*Adcy1*) that causes deficits in thalamocortical synapse development and the complete absence of barrels (Lu et al., 2003). Unlike ThVGdKO and ThMunc18KO mice, there was no difference in cortical lamination in *barrelless* mice in comparison to controls (Figures 4I–4N). These results suggest that cortical lamination defects, as observed in ThVGdKO and ThMunch18KO mice, occur as a consequence of the complete disruption of thalamocortical synaptic communication and are not a necessary consequence of simply disrupting barrel formation.

L4 Neurons Have Abnormal Pyramidal Morphology in ThVGdKO Mice

Changes in granular layer development suggest that neuronal differentiation of L4 neurons is disrupted in ThVGdKO mice. In rodent somatosensory cortex, most L4 excitatory neurons are spiny stellate cells, which are local circuit neurons with a small cell body and compact spiny dendrites (Simons and Woolsey, 1984; Lund, 1984). Spiny stellate neurons are largely confined to primary sensory areas of cortex and are common synaptic targets of thalamocortical axons (Benshalom and White, 1986). Mature L4 spiny stellate cells lack the apical process typical of pyramidal neurons in nongranular layers. Some studies suggest that the development of cortical L4 neuron morphology depends on sensory experience (Callaway and Borrell, 2011; Harris and Woolsey, 1981; McMullen et al., 1988). To investigate the role of thalamocortical glutamatergic neurotransmission on the development of spiny stellate cell morphology, we filled L4 cells with biocytin and digitally reconstructed their dendrites. We carefully limited our analysis to neurons that were confined to the bottom of the CUX1-positive band marking L4 of cortex. In P15 control mice (n = 25 neurons in four mice), L4 neurons expressed CUX1; had typical spiny

stellate morphology without an apical dendrite; and compact, asymmetric, spiny dendritic trees (Figure 5). In contrast, neurons in L4 of ThVGdKO mice (n = 36 from five mice) often did not express CUX1; had distinct apical dendrites that extended toward the pial surface, with large dendritic spans; relatively symmetric basal dendrites; and many fewer spines than control mice (Figures 5C–5E and 5H). Total dendritic length and the number of branch points were not significantly different in ThVGdKO and control neurons (Figures 5F and 5G). These results suggest that in the absence of thalamocortical glutamatergic neurotransmission, L4 development and the emergence of characteristic spiny stellate (granular cell) morphology are compromised.

Abnormal Expression of the L4 Marker *Dcdc2a* in ThVGdKO Mice

We next turned to molecular markers of cortical lamination to determine the extent of lamination defects in ThVGdKO mice. To depict L4 neurons in the somatosensory cortex, we used the *Dcdc2a-Gfp* transgenic reporter mouse generated by the GENSAT project (Gong et al., 2003). *Dcdc2a* is one of a family of genes containing two doublecortin domains, which bind tubulin and enhance microtubule polymerization (Kerjan and Gleeson, 2007). In humans, genetic variants in *DCDC2* have been associated with susceptibility to developmental dyslexia (Meng et al., 2005; McGrath et al., 2006), and functional analysis with *DCDC2* shRNA in rats suggests a role in neuronal migration during cortical development (Meng et al., 2005) that is partially redundant with doublecortin (*Dcx*; Wang et al., 2011). In *Dcdc2a-Gfp* mice, GFP is largely confined to L4 neurons in the barrel cortex and, to a lesser extent, L5a pyramidal shaped neurons that are distributed more broadly in the neocortex (Figures 6A and 6B). In ThVGdKO mice at P6, there were significantly fewer GFP positive cells than in control mice (Figures 6A and 6B), and most cells expressing GFP in ThVGdKO mice were arranged just below the dense band of CUX1 neurons in L4. This results in a significantly smaller fraction of GFP expressing neurons double-labeled with CUX1 in ThVGdKO mice relative to control mice (Figure 6C). At P15, the difference in expression was even more dramatic (Figures 6C and 6D), with many fewer neurons expressing GFP in ThGVdKO mice, and these cells were largely distributed deeper in cortex, corresponding to L5a, than in control mice and did not express CUX1 (Figure 6D). Thalamocortical axon terminal arbors at P15 completely overlapped with the layer of neurons expressing GFP (Figure 6E), consistent with the dominant expression of *Dcdc2a-Gfp* in L4 of control mice. In contrast, in ThVGdKO mice, GFP neurons were present mainly below the bulk of thalamocortical axon terminal arbors (Figure 6E). These data suggest that the normal maintenance in L4 and downregulation in L5a of *Dcdc2a* expression are disrupted in ThVGdKO mice, possibly due to disruptions in postnatal neuronal position or changes in laminar expression of the *Dcdc2a-Gfp* reporter.

Further Genetic Evidence of Lamination Defects in ThVGdKO Mice

We examined the expression of a number of genes with layer-specific expression patterns in ThVGdKO somatosensory cortex
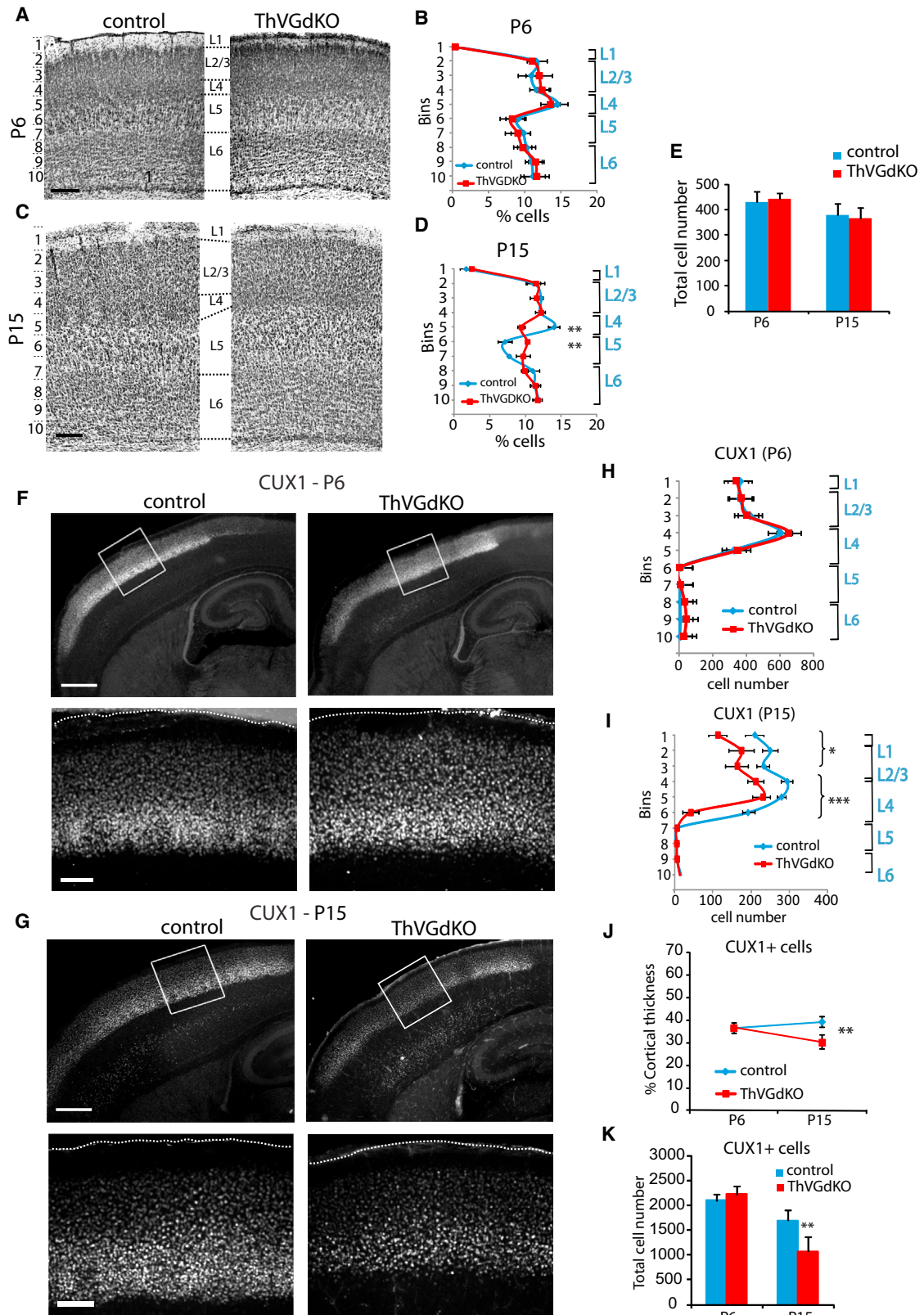
(legend on next page)

at P15 and consistently observed changes in and around L4. As already described, the expression of the predominantly superficial layer gene *Cux1* in ThVGdKO mice was significantly reduced (Figures 3G–3K), as was *SatB2* (Figures S5A and S5B). The expression of the L4 transcription factor *Rorb* (RORβ; Schaeren-Wiemers et al., 1997), and the L5a transcription factor *Etv1* (aka *Er81*; Yoneshima et al., 2006), changed reciprocally (Figures 7A–7D). In ThVGdKO, a dense band of *Rorb*-positive cells that corresponds to L4 was shifted upward (Figures 7A and 7B), consistent with the Nissl staining (Figures 3C and 3D). We also observed a number of *Rorb*-positive cells throughout L5 and L6 in ThVGdKO mice, which was more unusual in controls (Figure 7A, black arrows; Figures S6A and S6B, white arrows). In control mice, neurons expressing *Rorb* were mostly confined to L4 and coexpressed CUX1, whereas in ThVGdKO mice, *Rorb* expression extended to L5 where it was not coexpressed with CUX1 (Figure S7). The domain of *Etv1* expression spread toward the pial surface in ThVGdKO mice (Figures 7C and 7D), again consistent with the expansion of L5 observed with Nissl staining. The expression of L5b (*Ctip2*, *Fezf2*) and L6 (*FoxP2*, *Tbr1*) markers was largely undisturbed in the somatosensory cortex of ThVGdKO mice (Figures S5C–S5G, and data not shown), and changes in laminar-specific gene expression observed in somatosensory cortex did not occur in the motor cortex of ThVGdKO mice (Figures S6C and S6D). None of these aberrant expression patterns were apparent at P6 (Figure S6E). The changes in layer-specific gene expression observed in ThVGdKO cortex at P15 are consistent with the differences observed histologically and imply an unexpected degree of activity-dependent thalamic influence on laminar development of somatosensory cortex.

Changes in the Expression of Activity-Dependent Transcription Factors in ThVGdKO Mice

A number of transcription factors are regulated by activity in the cortex, particularly during experience-dependent circuit remodeling that occurs throughout development and in the adult (Flavell and Greenberg, 2008). We sought to examine whether such an activity-dependent signaling cascade might mediate the developmental changes we observed in the barrel cortex of ThVGdKO mice. The expression of FOS (c-Fos), a prototypical activity-dependent transcription factor, is dramatically

reduced in ThVGdKO mice in comparison to controls, particularly in superficial layers of cortex (Figures 7E and 7F). The *Egr* family of transcription factors is also regulated by activity during sensory cortex development (Mataga et al., 2001; Patra et al., 2004), and of the four known variants in the family (*Egr1–4*), the expression of EGR1 was significantly reduced in the superficial layers of somatosensory cortex of ThVGdKO mice (Figures 7G–7J; data not shown). Interestingly, *Cux1*, whose expression is reduced in superficial layers of ThVGdKO somatosensory cortex (Figures 3, 7I, and 7J), and *Etv1*, whose expression is increased (Figures 7C and 7D), both regulate dendritogenesis (Abe et al., 2012), dendrite branching, and spine morphology of pyramidal neurons in the upper layers of the cortex (Cubelos et al., 2010). This suggests that signaling mechanisms under the direct or indirect control of activity-dependent transcription factors may regulate late stages in the elaboration of cortical lamination and neuronal morphogenesis, particularly in L4 stellate cells of the somatosensory cortex.

DISCUSSION

We examined the role of neurotransmitter release by thalamocortical neurons on the emergence of distinct areal and laminar features during cortical development. Through the manipulation and elimination of vesicular glutamate from somatosensory thalamic nuclei, we identified a range of cortical attributes that depend on thalamocortical neurotransmission. In particular, the development of cortical "barrel" columns relied completely on glutamate released from thalamocortical neurons. Surprisingly, we also observed that aspects of cortical laminar cytoarchitecture and gene expression, particularly associated with the emergence of the "granular" L4, were disrupted in the absence of thalamocortical neurotransmission. Finally, the paucity of compact stellate (granular) cells and the persistence of pyramidal neuron dendritic morphology in L4 neurons of the somatosensory cortex of ThVGdKO mice indicate that the emergence of gross neuronal morphology is also influenced by activity-dependent factors. These results expand the apparent influence of neuronal activity in cortical development, suggesting that aspects of columnar development, lamination, and neuronal differentiation rely on thalamocortical neurotransmission.

Figure 3. Cortical Lamination Is Disrupted in ThVGdKO Somatosensory Cortex at P15

(A) Nissl-stained coronal sections through barrel cortex of control (left) and ThVGdKO mice (right) at P6. Scale bar represents 150 μm.

(B) Distribution of Nissl-stained cells as a function of depth (in indicated 100 μm bins from pial surface) at P6 (mean ± SEM). Controls, n = 5; ThVGdKO, n = 5.

(C) Nissl-stained coronal sections through the barrel cortex at P15. Scale bar represents 150 μm.

(D) Distribution of Nissl-stained cells as a function of depth (in indicated 150 μm bins from pial surface) at P15 (mean ± SEM). Controls, n = 13; ThVGdKO, n = 7. **p < 0.01. Note the significant difference in cell density at depths corresponding to L4 and upper L5.

(E) There was no difference in total cell number per barrel column at P6 and P15 between control and ThVGdKO mice (mean ± SEM).

(F) Representative images of CUX1 immunostaining in control and ThVGdKO somatosensory cortex at P6. Top: low-magnification images of thalamocortical sections. Bottom: high-magnification images of framed area in top panels. Scale bars represent 400 μm in top panel and 100 μm in bottom panel.

(G) Representative images of CUX1 immunostaining in control and ThVGdKO somatosensory cortex at P15. Top: low-magnification images of thalamocortical sections. Bottom: high-magnification images of framed area in top panels. Scale bars represent 400 μm in top panel and 100 μm in bottom panel.

(H) Distribution of CUX1+ cells as a function of depth in somatosensory cortex at P6 (mean ± SEM). For each group, n > 10.

(I) Distribution of CUX1+ cells as a function of depth in somatosensory cortex at P15 (mean ± SEM). For each group, n > 10; *p < 0.05; ***p < 0.001.

(J) CUX1+ cells form a similar fraction of cortical depth at P6 but decrease by P15 in ThVGdKO mice in comparison to controls (mean ± SEM), **p < 0.01.

(K) Total CUX1 cell number per barrel column at P15 (mean ± SEM). **p < 0.01. See also Figures S1, S2, and S3.
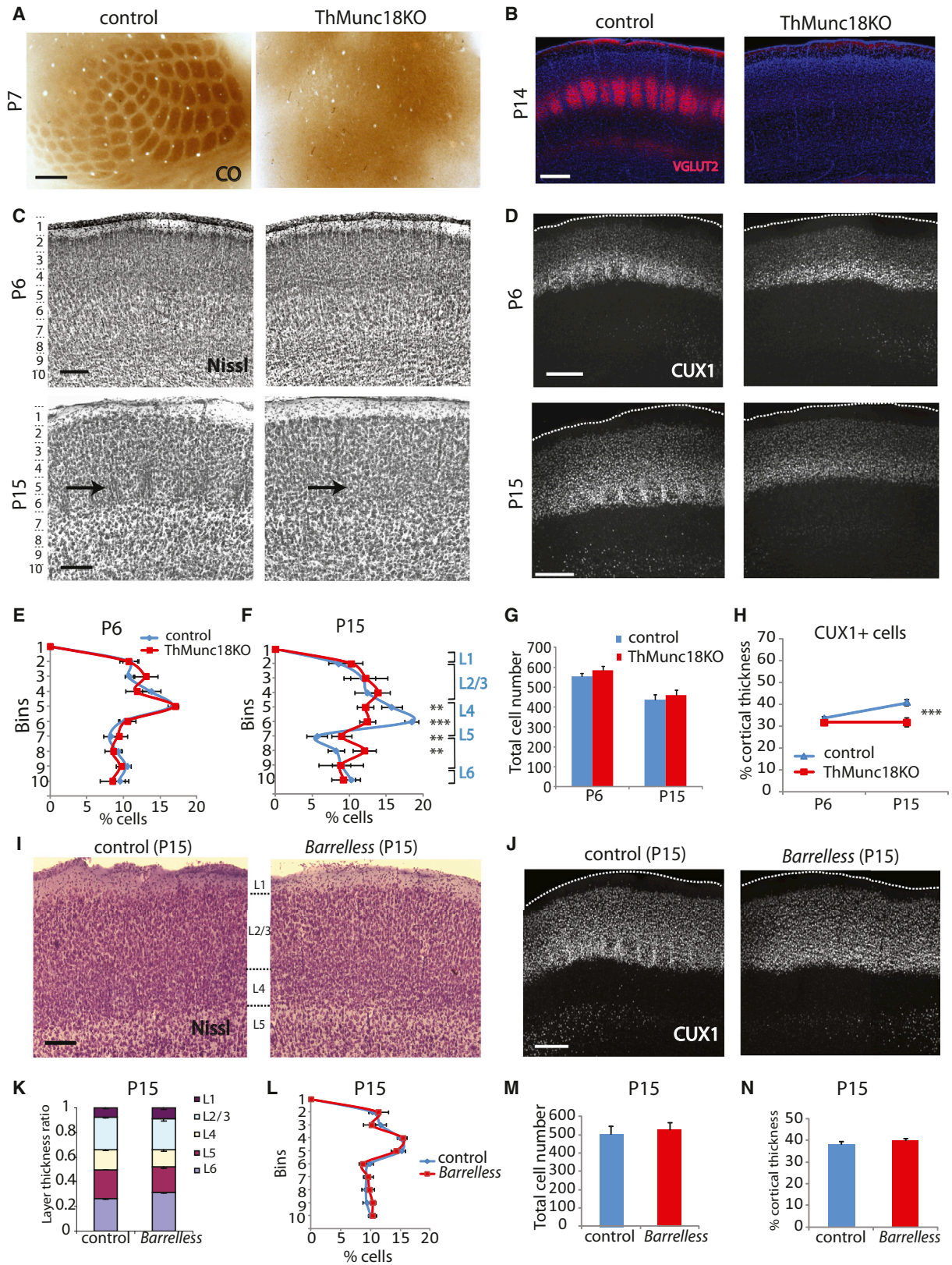
(legend on next page)

Barrel Development Requires Glutamate Release from Thalamocortical Neurons

Barrels are composed of cell sparse hollows filled with clusters of thalamocortical axon arbors surrounded by cell-dense walls of spiny stellate neurons. The dendrites of spiny stellate neurons that ring a barrel are oriented into the hollow to form synapses with thalamocortical afferents relaying information from a single whisker. Genetic mutations in mice that disrupt barrel development typically disrupt only the columnar distribution of neurons in L4 and leave the clustering of thalamocortical axons intact (Li and Crair, 2011). A handful of the most severe barrel map mutants, including *barrelless* mice and GAP-43 KO mice, have no hint of either thalamocortical axon clustering into barrels or L4 cytoarchitecture resembling barrel walls. Previous experiments that disrupted neuronal activity or cortical glutamatergic signaling pharmacologically or genetically had mixed effects on barrel development (Li and Crair, 2011). For instance, interfering with cortical glutamatergic receptors (Schlaggar et al., 1993; Iwasato et al., 2000; Wijetunge et al., 2008) disrupts cortical barrel cytoarchitecture, but has no effect on thalamocortical axon clustering into a barrel pattern. Similarly, interfering with neuronal activity pharmacologically (Chiaia et al., 1992) or disrupting thalamocortical neurotransmission genetically (Lu et al., 2006; Narboux-Nême et al., 2012) interferes with the emergence of cortical barrel cytoarchitecture but has no effect on thalamocortical axon clustering. Notably however, the interventions used in these studies did not completely block thalamocortical glutamatergic neurotransmission, but rather interfered with restricted subsets of glutamate receptors or decreased the probability of neurotransmitter release without eliminating thalamocortical neurotransmission or changing synaptic strength. A likely consequence of the incomplete nature of these manipulations is that barrel cytoarchitecture is disrupted, but thalamocortical axon clustering and cortical laminar cytoarchitecture are preserved. In contrast to these previous studies, the manipulation we reported here nearly completely blocks thalamocortical neurotransmission (ThMunc18KO mice) or nearly completely prevents thalamocortical neurons from releasing glutamate (ThVGdKO mice). We suggest that the more comprehensive disruption of thalamocortical glutamatergic neurotransmission we achieved produced the correspondingly more dramatic effects on cortical barrel, laminar, and neuronal cytoarchitectural development.

We observed that *Vglut1* was capable of compensating for the absence of *Vglut2* in thalamocortical neurons in vivo. The same is not true in cultured neurons, where thalamic cells that lack only *Vglut2* have dramatically disrupted neurotransmitter release (Moechars et al., 2006). Neurons in the ventrobasal thalamus are known to express both *Vglut1* and *Vglut2* in a dynamic fashion through the course of development (Barroso-Chinea et al., 2008; Nakamura et al., 2005), as do single axon terminals in L4 of barrel cortex during the first week after birth (Nakamura et al., 2005). The observed difference in compensation by *Vglut1* for *Vglut2* may reflect a difference in the dynamic regulation of these two *Vglut* gene family members in vivo and in vitro.

Defects in Cortical Lamination in Somatosensory Cortex of ThVGdKO Mice

It is notable that the initial wave of cortical lamination and lamina-specific gene expression that occurs through the first week after birth appears largely normal in ThVGdKO and ThMunc18KO mice, which suggests that initial migration cues guiding cells from the ventricular zone to the pial surface are intact in ThVGdKO and ThMunc18KO mice, but local cues responsible for distributing neurons into barrel walls (columns) are disrupted. This is consistent with previous studies in mice lacking extrinsic connections (Miyashita-Lin et al., 1999; Zhou et al., 2010) or after thalamic ablation (Windrem and Finlay, 1991) and conforms with a classic "protomap" view of development in which cortical development (arealization and lamination) is self-organized (Rakic et al., 2009), but specific local features of cortical

---

Figure 4. Cortical Lamination Is Disrupted in ThMunc18KO but Not *Barreless* Mice at P15

(A) CO histochemistry shows that barrels do not form in ThMunc18KO mice (right). Scale bar represents 200 μm.

(B) Immunostaining for VGLUT2 reveals that thalamocortical axons do not innervate barrel cortex in ThMunc18KO mice at P14 (right). Scale bar represents 300 μm.

(C) Nissl histochemistry shows that cortical lamination in ThMunc18KO somatosensory cortex (top right) at P6 is similar to controls (top left). Scale bar represents 150 μm. By P15, cortical lamination in ThMunc18KO somatosensory cortex (bottom right) is disrupted in comparison to controls (bottom left). Scale bar represents 150 μm.

(D) CUX1 immunostaining of somatosensory cortex in ThMunc18KO mice at P6 (top right) and controls (top left) is similar. By P15, CUX1 labeled cells form a smaller fraction of the cortical depth in ThMunc18KO mice (bottom right) in comparison to controls (bottom left). Scale bar represents 200 μm.

(E) Quantification of laminar distribution of Nissl-stained cells in control and ThMunc18KO mice at P6. Data presented as mean ± SEM; n = 4 for each genotype.

(F) Quantification of laminar distribution of Nissl-stained cells in control and ThMunc18KO mice at P15. Data presented as mean ± SEM. **p < 0.01, ***p < 0.001, n = 4 for ThMunc18KO, n = 6 for controls.

(G) Total number of Nissl-stained cells per barrel column in ThMunc18KO and littermate controls at P6 and P15 (mean ± SEM).

(H) CUX1+ cells form a similar fraction of the total cortical thickness at P6 but a smaller fraction at P15 in Munc18KO mice in comparison to controls (mean ± SEM). ***p < 0.001.

(I) Nissl histochemistry shows that cortical lamination in somatosensory cortex is similar in *Barreless* mice (right) and controls (left), with the obvious exception that barrels are absent in *Barreless*. Scale bar represents 150 μm.

(J) CUX1 immunostaining of somatosensory cortex in *Barreless* (right) mice and controls (left) is similar. Scale bar represents 200 μm.

(K) The laminar distribution of Nissl-stained cells as a fraction of total thickness in *Barreless* and control somatosensory cortex at P15 is similar.

(L) The laminar distribution of Nissl-stained cells as a function of depth in *Barreless* and control somatosensory cortex at P15 is similar.

(M) Total number of Nissl-stained cells per barrel column in somatosensory cortex is similar in *Barreless* and control mice.

(N) The fraction of barrel cortex thickness covered by CUX1-positive cells is similar in *Barreless* and control somatosensory cortex.

See also Figure S4.
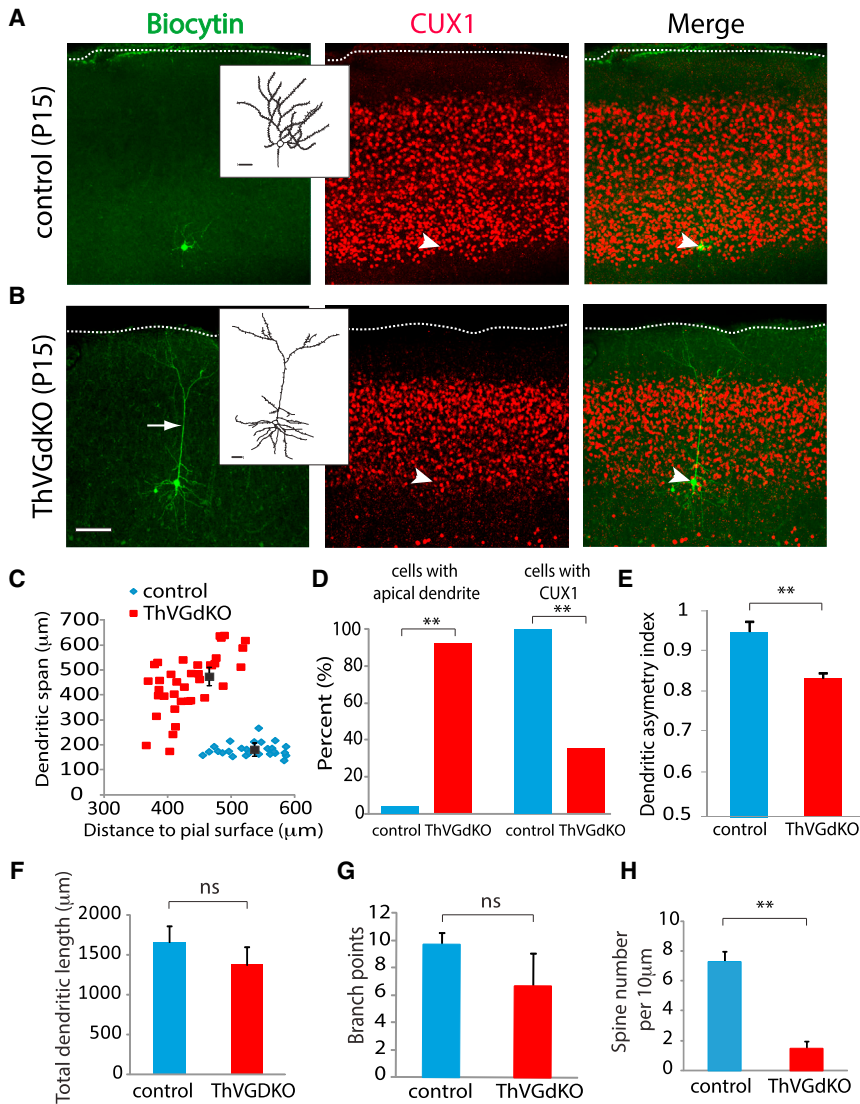
Figure 5. Neurons in L4 of ThVGdKO Mice Have Pyramidal, Not Granular Morphology

(A) Representative biocytin-filled L4 spiny stellate neuron in control animal (left). Inset shows digitally reconstructed dendritic tree. Immunostaining for CUX1 (center) was used to identify the laminar location of the filled cell. Merged image is on the right. Arrowhead indicates position of the filled neuron. Scale bar represents 100 μm, 30 μm for inset.

(B) Representative biocytin-filled L4 neuron in ThVGdKO animal (left). Arrow shows an apical dendrite that extends all the way to the pial surface. Inset shows digitally reconstructed dendritic tree. Immunostaining for CUX1 (center) was used to identify the laminar location of the filled cell. Merged image is on the right. Arrowhead indicates position of the filled neuron. Only neurons in the lower band of CUX1 immunostain (within 150 μm of the lower edge) were considered for further analysis. Scale bar represents 100 μm, 30 μm for inset.

(C) The dendritic span of reconstructed neurons in ThVGdKOs is significantly greater than that in controls. Note that the dendritic span is consistently small for control animals, regardless of the cortical depth of the labeled neuron, while the dendritic span in ThVGdKO mice is larger for neurons that are deeper, consistent with an apical dendrite that extends to the pial surface regardless of depth. From five animals in ThVGdKO, n = 36 neurons; from four control animals, n = 25 neurons.

(D) Only 1 of 25 neurons in L4 of control mice had an apical dendrite, while 32 of 36 neurons in ThVGdKO had a distinct apical dendrite. Twenty-five of 25 L4 neurons in control mice expressed CUX1, while only 13 of 36 neurons in ThVGdKO mice expressed CUX1.

(E) Dendrites in L4 neurons in ThVGdKO mice are more symmetric than control neurons; **p < 0.01.

(F) Total dendritic length in ThVGdKO mice is not significantly different from that in controls (mean ± SEM).

(G) The number of dendritic branch points in ThVGdKO mice is not significantly different from that in controls (mean ± SEM).

(H) Spine density in ThVGdKO L4 neurons is significantly lower in ThVGdKO relative to that in control mice (mean ± SEM).

patterning (barrel columns) are sensitive to extrinsic influences. Subsequent to the initial wave of normal migration, the elaboration of superficial cortical lamina and lamina-specific gene expression in the second week after birth is markedly disrupted in ThVGdKO and ThMunc18KO mice. These defects may be due to "local" positioning errors, analogous to the errors that produce barrel wall defects, and/or a disruption in the morphologic and molecular elaboration of superficial layer neuron identity, particularly in L4. The elaboration of features of cortical organization that emerge during the second postnatal week may be much more sensitive to the influence of extrinsic factors, such as thalamocortical activity, which is more consistent with a classic "protocortex" view of development (O'Leary, 1989). The deficits in barrel formation, superficial cortical lamination, and neuronal morphological development apparent in ThVGdKO mice provide

a clear demarcation between specific features of cortical development that are dependent on extrinsic, activity-dependent influences and features of cortical development that are principally self-organizing.

It is also notable that the cortical lamination defects we observed in ThVGdKO mice appear restricted to somatosensory cortex and do not encompass other cortical areas with distinct granular layers (L4), such as the auditory cortex and the visual cortex. We believe this is due to the significantly more effective deletion of *Vglut2* from somatosensory thalamus (VB) than the visual thalamus (dLGN) or auditory thalamus (MGN) in ThVGdKO mice (Figure S3). It is also possible that there is something unique about the somatosensory cortex that makes it more sensitive to the elimination of glutamate release from thalamocortical neurons. For instance, the
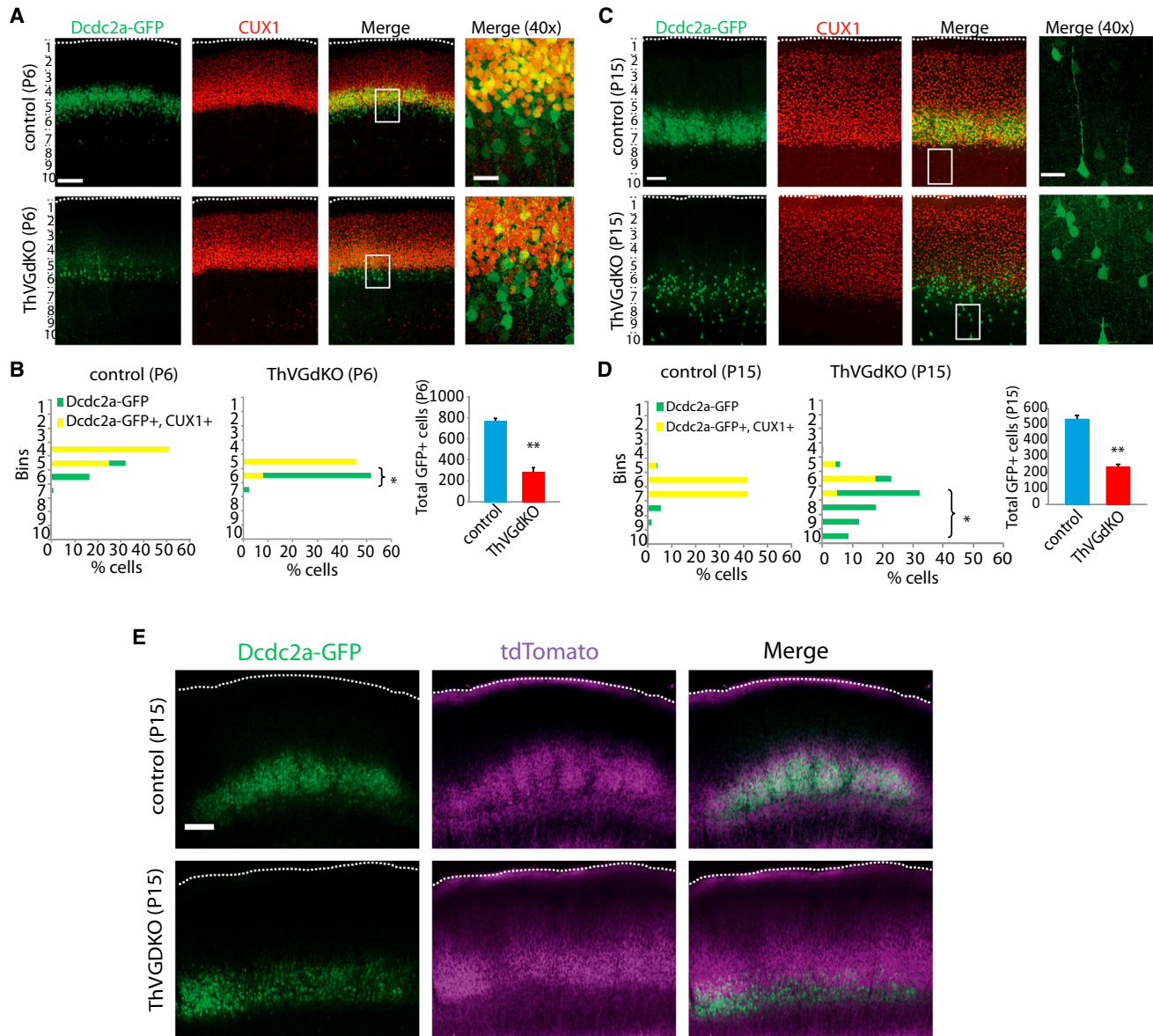
Figure 6. Laminar Distribution of Dcdc2a-GFP Neurons Is Altered in ThVGdKO Mice

(A) In control mice at P6 (top), *Dcdc2a-GFP+* cells are distributed at the bottom edge and largely colocalized with CUX1 expressing neurons in somatosensory cortex. In ThVGdKO mice at P6 (bottom), there are fewer *Dcdc2a-GFP+* cells, and these cells tend to reside below the layer of CUX1-expressing neurons. Scale bar represents 100 μm; 20 μm for 40× pictures.

(B) Quantification of laminar distribution of *Dcdc2a-GFP+* cells in somatosensory cortex at P6. Total number of GFP+ cells (right panel) is significantly reduced at P6 (mean ± SEM). **p < 0.01 and n = 3 for each genotype.

(C) At P15, the difference between ThVGdKO mice and control mice is more striking, with many fewer *Dcdc2a-GFP+* neurons in ThVGdKO mice (bottom) in comparison to control mice (top), and these neurons are below the CUX1 layer and do not colocalize with CUX1. Scale bar represents 100 μm, 20 μm for 40× pictures.

(D) Quantification of laminar distribution of *Dcdc2a-GFP+* cells in somatosensory cortex of control (left) and ThVGdKO mice (middle). Total number of *Dcdc2a-GFP+* cells (right) is significantly reduced at P15 (mean ± SEM). *p < 0.05; **p < 0.01, and n = 3 for each genotype.

(E) In control mice at P15 (top), dcdc2aGFP-expressing neurons (left) largely overlap with thalamocortical afferent arbors (middle) in L4. In contrast, in ThVGdKO mice (bottom) *Dcdc2a-GFP*-expressing neurons (left) and thalamocortical arbors labeled with tdTomato (middle) overlap weakly (right). Scale bar represents 200 μm. See also Figure S5.

development of the auditory cortex and the visual cortex are delayed relative to the somatosensory cortex by a few days, but this difference would not appear to be substantial enough to account for the absence of a lamination phenotype in these cortical areas at P15, when cortical elaboration should be reasonably complete everywhere.
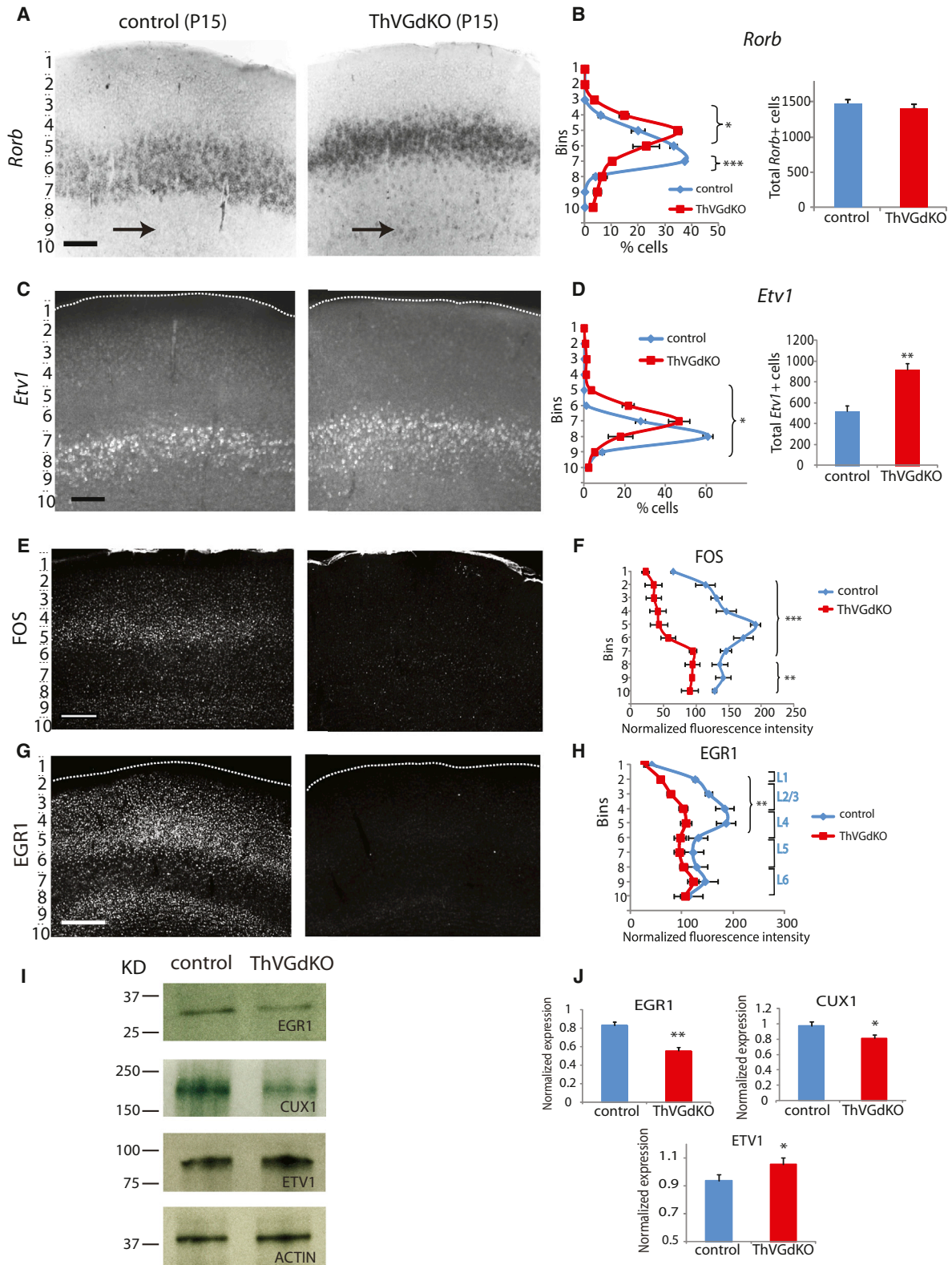
Figure 7. Changes in L4 and L5 Molecular Markers in ThVGdKO Mice

(A) In situ hybridization for *Rorb* at P15 shows a dense band of labeled cells that is shifted toward the pial surface in ThVGdKO mice (right) relative to controls (left). Arrows mark sparse L5 cells, which are more prominent in ThVGdKO mice. Scale bar represents 150 μm.

(legend continued on next page)

Requirement of Thalamic Glutamate for Development of L4 Spiny Stellate Morphology

The compact, "granular" morphology of L4 is a characteristic feature of mammalian sensory cortex (Staiger et al., 2004). The typical spiny stellate (granular) morphology of L4 excitatory neurons is thought to arise from a common cortical pyramidal cell template after the elimination of a developmentally precocious pial-projecting apical dendrite (Callaway and Borrell, 2011). The conspicuous absence of spiny stellate neurons in ThVGdKO mice and the persistence of pyramidal-like L4 cells with apical dendrites that extend to the pial surface are consistent with a model in which cortical excitatory neurons adopt a pyramidal cell morphology by default (Lu et al., 2013), and the emergence of spiny stellate morphology is an activity-dependent process under thalamic guidance (Callaway and Borrell, 2011). This is a clear example of the morphologic development of a distinct cell type typical of only one cortical layer that is regulated by thalamus-derived factors (Sato et al., 2012; Lombardo et al., 1995), presumably through a transcription factor expression cascade under the direct or indirect influence of thalamocortical activity. Similar activity-dependent transcription factor cascades may account for aspects of the distinct laminar, neuronal, and circuit wiring properties characteristic of different areas of neocortex.

Activity-Dependent Expression of Laminar and Molecular Markers

Recent experiments indicate that a wide number and variety of genes in the brain are transcribed in an activity-dependent manner (Kim et al., 2010). Activity-regulated gene transcription is important for synapse formation (West and Greenberg, 2011), axon branching (Hayano and Yamamoto, 2008), dendritic development (Whitford et al., 2002), and even interneuron migration and development (De Marco García et al., 2011). The results described here suggest that the positioning and morphologic development of cortical glutamatergic neurons is also subject to activity-dependent regulation under the specific influence of the thalamus. We observed that genes typically associated with granular and supragranular layers, such as *Cux1* and *Satb2*, have reduced expression in ThVGdKO mice, while genes typically expressed in the deepest layers of cortex, such as *Bcl11b* (aka *Ctip2*), *Fezf2* (aka *Fezl, Zfp312*), and *FoxP2* were not altered in ThVGdKO mice. Genes normally enriched in L5a neurons, such as *Etv1*, were increased in ThVGdKO mice, and many cells in L5 spuriously coexpressed *Rorb*, typically associ-

ated with L4. Interestingly, the expression of *Tbr1*, a transcription factor that is mainly expressed in L6 but also expressed to a lesser extent in L4, is increased in L4 but not in L6 of ThVGdKO mice (Figure S5). Thus, it appears that the expression and distribution of genes in and around L4 of ThVGdKO somatosensory cortex is specifically altered, presumably as a consequence of changes in activity-dependent transcriptional regulation. For example, we observed that the immediate early gene *Egr1*, which binds to the promoter for *Cux1* (Champion ChiP Transcription Factor Search Portal, http://www.sabiosciences.com/chipqpcrsearch.php), is suppressed in ThVGdKO mice (Figure 7). In turn, *Cux1* has multiple binding sites on *Etv1* and may act as a transcriptional repressor. *Etv1* is spuriously expressed in L4 neurons of ThVGdKO mice (Figures 7C and 7D) and is known to regulate dendritogenesis (Abe et al., 2012), which is atypical in L4 neurons in ThVGdKO mice (Figure 5). This and/or other activity-dependent signaling mechanisms or transcription factors, including *Fos,* may regulate late stages of lamination and neuronal morphogenesis, particularly for stellate cells in L4 of the somatosensory cortex.

How Does Thalamocortical Glutamate Act to Modulate Barrel Cortex Development?

We favor a model in which thalamocortical neurons convey the arrangement of whiskers on the snout to the cortex to form barrels in L4 through the effect of their correlated pattern of activity on the development of granular (spiny stellate) neurons. Similarly, alterations in cortical lamination observed in ThVGdKO mice are a consequence of the elimination of the glutamatergic synaptic drive on developing L4 neurons. In this model, glutamate acts directly at thalamocortical synapses of spiny stellate neurons to modulate activity and direct the local migration of neurons into barrels, modify gene expression, and influence cell morphologic development. We suggest that the gradual emergence of a laminar and cell morphologic phenotype in the second week after birth in ThMunc18KO and ThVGdKO mice reflects the progressive nature of cortical development that becomes increasingly influenced by activity as the brain matures, rather than a frank "respecification" of neuron laminar or morphologic identity. Alternatively, respecification (or "fate conversion") of postmitotic superficial layer neurons may occur in the absence of glutamatergic drive from the thalamus even as late as the first postnatal week (De la Rossa et al., 2013).

(B) Quantitative analysis of the laminar distribution of *Rorb+* cells across layers (mean ± SEM) shows that the dense band of *Rorb+* cells is shifted upward and there are an increased number of *Rorb+* cells in deeper layers in ThVGdKO somatosensory cortex. The total number of *Rorb+* cells is not different in the two genotypes (right). *p < 0.05; ***p < 0.001, and n = 4 for each genotype.

(C) In situ hybridization for *Etv1* at P15 in ThVGdKO (right) and littermate control (left) mice. Scale bar represents 150 μm.

(D) The laminar distribution of *Etv1+* cells in ThVGdKO mice is shifted toward the pial surface relative to control mice, and there are many more *Etv1+* cells in ThVGdKO mice (mean ± SEM). *p < 0.05; **p < 0.01, and n = 5 for each genotype.

(E) C-FOS expression is dramatically reduced in ThVGdKO mice (right) relative to control mice (left) at P14.

(F) Laminar distribution of FOS expression (mean ± SD) shows reduced expression throughout cortex, particularly in superficial layers. ***p < 0.001; **p < 0.01, and n = 2.

(G) EGR1 immunostaining in somatosensory cortex of ThVGdKO (right) and littermate controls (left) at P15. Scale bar represents 300 μm.

(H) EGR1 expression is reduced in ThVGdKO mice relative to littermate control mice, particularly in superficial layers (mean ± SEM). **p < 0.01.

(I) Western blot analysis shows that EGR1 and CUX1 expression are reduced in ThVGdKO somatosensory cortex, while ETV1 expression is increased.

(J) Quantification of western blots for indicated proteins. *p < 0.05; **p < 0.01, n = 3 for controls and ThVGdKOs.

See also Figures S6 and S7.

The experimental manipulation we performed blocked glutamate release from thalamocortical neurons, but did not specifically modulate neuronal activity or exclusively synaptic activity. For instance, glutamate receptors expressed in glial cells or extrasynaptically in neurons could potentially cause the phenotypes we observed. Moreover, activity throughout barrel cortex is likely reduced in the absence of glutamatergic drive by thalamocortical axons onto L4 neurons in ThVGdKO mice. It is possible that extrasynaptic glutamate or altered activity patterns throughout the cortex mediate the effects on barrel cortex development we observed in ThVGdKO mice. In any case, the striking effects of eliminating thalamocortical neurotransmitter release on cortical columnar, laminar, and neuronal morphologic development suggests that these events are modulated by factors extrinsic to the cortex that are sensitive to ongoing thalamic activity. These extrinsic factors may play a role in the emergence of areal differences seen in the cortex during normal development, such as the presence of a dense granular L4 in the sensory cortex and an expanded L5 in the motor cortex. Thus, abnormal patterns of activity during development, or disruptions in activity-dependent transcription factor cascades, may account for some of the laminar, morphologic, and synaptic defects observed in a variety of neurodevelopmental disorders.

EXPERIMENTAL PROCEDURES

Animals

All animals were treated in compliance with Yale IACUC and U.S. Department of Health and Human Services guidelines. We maintained and bred *Sert-Cre*$^{+/-}$;*Vglut1*$^{+/-}$;*Vglut2*$^{fl/+}$, *Sert-Cre*$^{+/-}$;*Vglut1*$^{+/-}$;*Vglut2*$^{fl/-}$, and *Vglut1*$^{+/-}$;*Vglut2*$^{fl/fl}$ mice on a mixed C57B/6J and CD1 background and used *Vglut1*$^{-/-}$;*Vglut2*$^{fl/-}$ mice as littermate controls for ThVGdKO (*Sert-Cre*$^{+/-}$;*vglut1*$^{-/-}$;*vglut2*$^{fl/fl}$, and *Sert-Cre*$^{+/-}$;*Vglut1*$^{-/-}$;*Vglut2*$^{fl/-}$) mice throughout unless otherwise explicitly stated. *Dcdc2a-Gfp* and *Fezf2-Gfp* transgenic mice were obtained from GENSAT.

Histology

As previously described (Iwasato et al., 2008), CO and Nissl stain was performed on flattened tangential sections through the barrel cortex. CO was depicted using a solution of 3 mg cytochlomec, 0.4 g sucrose, and one 3,3′-diaminobenzidine tablet (Sigma) in 10 ml PBS. Nissl bodies were depicted with a 2% cresyl violet solution. Stereologic quantification of Nissl sections was performed on mounted slides at high magnification (40× or 63×) with Neurolucida Software (MicroBrightfield) blind to genotype. Statistical analysis was performed with two-tailed Student's t tests and one-way ANOVA. Significance level was set at p < 0.05. One microliter of Cre-dependent AAV2/9 CAG.FLEX.tdTomato.WPRE.bGH virus (University of Pennsylvania Vector Core Cat AV-9-ALL864) was injected into the thalamus using a Nanoject (Drummond Scientific) for demonstration of thalamocortical afferents with tdTomato. Biocytin labeling of L4 neurons was performed on acute thalamocortical slices using whole-cell patch pipettes that contained 10 mM Biocytin in addition to the standard whole cell solution. Labeled neurons were depicted with confocal and multiphoton laser microscopy (LSM duo710, Zeiss) and reconstructed using Neurolucida (MBF Bioscience). In situ hybridization was performed with Digoxigenin-11-UTP and/or Fluorescence-12-UTP (Roche) probes on 60 μm free-floating coronal sections. Immunohistochemistry was performed on free-floating 60-μm-thick thalamocortical or coronal sections, and images for fluorescence quantification were acquired with a Zeiss Axio Imager.Z2 or LSM 510 Meta microscope using the same exposure time and background subtraction for all genotypes. Quantification of laminar distribution was performed on images with the pial surface at the upper edge and the cortex depth divided into ten equal bins below the pial surface. Cells in each bin were counted using ImageJ (NIH) and Volocity (PerkinElmer) software and reported as a percentage of total cells counted blind to genotype. Statistical analysis was performed with two-tailed Student's t tests and one-way ANOVA with significance level set at p < 0.05.

Electrophysiology

In vitro whole-cell patch-clamp electrophysiology was performed on acute thalamocortical brain slices as previously described (Lu et al., 2001). AMPA "evoked mini-EPSCs" were recorded at −70 mV holding potential after the exchange of Ca^{2+} for Sr^{2+}in the ACSF, and mini-EPSCs were analyzed with Mini Analysis (Synaptosoft). In vivo electrophysiology was performed on P9–P12 mice using a 16-site linear silicon probe (NeuroNexus Technologies) and analyzed using Spike2 (Cambridge Electronic Design). Whisker stimulation with puffs of air was applied using a Picospritzer III (Parker).

SUPPLEMENTAL INFORMATION

Supplemental Information includes Supplemental Experimental Procedures and seven figures and can be found with this article online at http://dx.doi.org/10.1016/j.neuron.2013.06.043.

REFERENCES

Abe, H., Okazawa, M., and Nakanishi, S. (2012). Gene regulation via excitation and BDNF is mediated by induction and phosphorylation of the Etv1 transcription factor in cerebellar granule cells. Proc. Natl. Acad. Sci. USA *109*, 8734–8739.

Barroso-Chinea, P., Castle, M., Aymerich, M.S., and Lanciego, J.L. (2008). Expression of vesicular glutamate transporters 1 and 2 in the cells of origin of the rat thalamostriatal pathway. J. Chem. Neuroanat. *35*, 101–107.

Benshalom, G., and White, E.L. (1986). Quantification of thalamocortical synapses with spiny stellate neurons in layer IV of mouse somatosensory cortex. J. Comp. Neurol. *253*, 303–314.

Callaway, E.M., and Borrell, V. (2011). Developmental sculpting of dendritic morphology of layer 4 neurons in visual cortex: influence of retinal input. J. Neurosci. *31*, 7456–7470.

Chiaia, N.L., Fish, S.E., Bauer, W.R., Bennett-Clarke, C.A., and Rhoades, R.W. (1992). Postnatal blockade of cortical activity by tetrodotoxin does not disrupt the formation of vibrissa-related patterns in the rat's somatosensory cortex. Brain Res. Dev. Brain Res. *66*, 244–250.

Crair, M.C., and Malenka, R.C. (1995). A critical period for long-term potentiation at thalamocortical synapses. Nature *375*, 325–328.

Cubelos, B., Sebastián-Serrano, A., Beccari, L., Calcagnotto, M.E., Cisneros, E., Kim, S., Dopazo, A., Alvarez-Dolado, M., Redondo, J.M., Bovolenta, P., et al. (2010). Cux1 and Cux2 regulate dendritic branching, spine morphology, and synapses of the upper layer neurons of the cortex. Neuron *66*, 523–535.

De la Rossa, A., Bellone, C., Golding, B., Vitali, I., Moss, J., Toni, N., Lüscher, C., and Jabaudon, D. (2013). In vivo reprogramming of circuit connectivity in postmitotic neocortical neurons. Nat. Neurosci. *16*, 193–200.

De Marco García, N.V., Karayannis, T., and Fishell, G. (2011). Neuronal activity is required for the development of specific cortical interneuron subtypes. Nature *472*, 351–355.

Dudok, J.J., Groffen, A.J.A., Toonen, R.F.T., and Verhage, M. (2011). Deletion of Munc18-1 in 5-HT neurons results in rapid degeneration of the 5-HT system and early postnatal lethality. PLoS ONE 6, e28137.

Flavell, S.W., and Greenberg, M.E. (2008). Signaling mechanisms linking neuronal activity to gene expression and plasticity of the nervous system. Annu. Rev. Neurosci. 31, 563–590.

Fremeau, R.T., Jr., Voglmaier, S., Seal, R.P., and Edwards, R.H. (2004). VGLUTs define subsets of excitatory neurons and suggest novel roles for glutamate. Trends Neurosci. 27, 98–103.

Gong, S., Zheng, C., Doughty, M.L., Losos, K., Didkovsky, N., Schambra, U.B., Nowak, N.J., Joyner, A., Leblanc, G., Hatten, M.E., and Heintz, N. (2003). A gene expression atlas of the central nervous system based on bacterial artificial chromosomes. Nature 425, 917–925.

Grove, E.A., and Fukuchi-Shimogori, T. (2003). Generating the cerebral cortical area map. Annu. Rev. Neurosci. 26, 355–380.

Harris, R.M., and Woolsey, T.A. (1981). Dendritic plasticity in mouse barrel cortex following postnatal vibrissa follicle damage. J. Comp. Neurol. 196, 357–376.

Hayano, Y., and Yamamoto, N. (2008). Activity-dependent thalamocortical axon branching. Neuroscientist 14, 359–368.

Hensch, T.K. (2004). Critical period regulation. Annu. Rev. Neurosci. 27, 549–579.

Hnasko, T.S., Chuhma, N., Zhang, H., Goh, G.Y., Sulzer, D., Palmiter, R.D., Rayport, S., and Edwards, R.H. (2010). Vesicular glutamate transport promotes dopamine storage and glutamate corelease in vivo. Neuron 65, 643–656.

Huberman, A.D., Feller, M.B., and Chapman, B. (2008). Mechanisms underlying development of visual maps and receptive fields. Annu. Rev. Neurosci. 31, 479–509.

Iwasato, T., Datwani, A., Wolf, A.M., Nishiyama, H., Taguchi, Y., Tonegawa, S., Knöpfel, T., Erzurumlu, R.S., and Itohara, S. (2000). Cortex-restricted disruption of NMDAR1 impairs neuronal patterns in the barrel cortex. Nature 406, 726–731.

Iwasato, T., Inan, M., Kanki, H., Erzurumlu, R.S., Itohara, S., and Crair, M.C. (2008). Cortical adenylyl cyclase 1 is required for thalamocortical synapse maturation and aspects of layer IV barrel development. J. Neurosci. 28, 5931–5943.

Kerjan, G., and Gleeson, J.G. (2007). Genetic mechanisms underlying abnormal neuronal migration in classical lissencephaly. Trends Genet. 23, 623–630.

Kim, T.-K., Hemberg, M., Gray, J.M., Costa, A.M., Bear, D.M., Wu, J., Harmin, D.A., Laptewicz, M., Barbara-Haley, K., Kuersten, S., et al. (2010). Widespread transcription at neuronal activity-regulated enhancers. Nature 465, 182–187.

Kwan, K.Y., Sestan, N., and Anton, E.S. (2012). Transcriptional co-regulation of neuronal migration and laminar identity in the neocortex. Development 139, 1535–1546.

Lebrand, C., Cases, O., Wehrlé, R., Blakely, R.D., Edwards, R.H., and Gaspar, P. (1998). Transient developmental expression of monoamine transporters in the rodent forebrain. J. Comp. Neurol. 401, 506–524.

Li, H., and Crair, M.C. (2011). How do barrels form in somatosensory cortex? Ann. N Y Acad. Sci. 1225, 119–129.

Lombardo, A., Rabacchi, S.A., Cremisi, F., Pizzorusso, T., Cenni, M.C., Possenti, R., Barsacchi, G., and Maffei, L. (1995). A developmentally regulated nerve growth factor-induced gene, VGF, is expressed in geniculocortical afferents during synaptogenesis. Neuroscience 65, 997–1008.

Lu, H.-C., Gonzalez, E., and Crair, M.C. (2001). Barrel cortex critical period plasticity is independent of changes in NMDA receptor subunit composition. Neuron 32, 619–634.

Lu, H.-C., She, W.-C., Plas, D.T., Neumann, P.E., Janz, R., and Crair, M.C. (2003). Adenylyl cyclase I regulates AMPA receptor trafficking during mouse cortical 'barrel' map development. Nat. Neurosci. 6, 939–947.

Lu, H.-C., Butts, D.A., Kaeser, P.S., She, W.C., Janz, R., and Crair, M.C. (2006). Role of efficient neurotransmitter release in barrel map development. J. Neurosci. 26, 2692–2703.

Lu, W., Bushong, E.A., Shih, T.P., Ellisman, M.H., and Nicoll, R.A. (2013). The cell-autonomous role of excitatory synaptic transmission in the regulation of neuronal structure and function. Neuron 78, 433–439.

Lund, J.S. (1984). Spiny stellate neurons. In Cerebral Cortex, Volume 1: Cellular Components of the Cerebral Cortex, A. Peters and E.G. Jones, eds. (New York:: Springer), pp. 255–308.

Mataga, N., Fujishima, S., Condie, B.G., and Hensch, T.K. (2001). Experience-dependent plasticity of mouse visual cortex in the absence of the neuronal activity-dependent marker egr1/zif268. J. Neurosci. 21, 9724–9732.

McGrath, L.M., Smith, S.D., and Pennington, B.F. (2006). Breakthroughs in the search for dyslexia candidate genes. Trends Mol. Med. 12, 333–341.

McMullen, N.T., Goldberger, B., Suter, C.M., and Glaser, E.M. (1988). Neonatal deafening alters nonpyramidal dendrite orientation in auditory cortex: a computer microscope study in the rabbit. J. Comp. Neurol. 267, 92–106.

Meng, H., Smith, S.D., Hager, K., Held, M., Liu, J., Olson, R.K., Pennington, B.F., DeFries, J.C., Gelernter, J., O'Reilly-Pol, T., et al. (2005). DCDC2 is associated with reading disability and modulates neuronal development in the brain. Proc. Natl. Acad. Sci. USA 102, 17053–17058.

Miyashita-Lin, E.M., Hevner, R., Wassarman, K.M., Martinez, S., Rubenstein, J.L., and Rubenstein, J.L. (1999). Early neocortical regionalization in the absence of thalamic innervation. Science 285, 906–909.

Moechars, D., Weston, M.C., Leo, S., Callaerts-Vegh, Z., Goris, I., Daneels, G., Buist, A., Cik, M., van der Spek, P., Kass, S., et al. (2006). Vesicular glutamate transporter VGLUT2 expression levels control quantal size and neuropathic pain. J. Neurosci. 26, 12055–12066.

Molyneaux, B.J., Arlotta, P., Menezes, J.R.L., and Macklis, J.D. (2007). Neuronal subtype specification in the cerebral cortex. Nat. Rev. Neurosci. 8, 427–437.

Nakamura, K., Hioki, H., Fujiyama, F., and Kaneko, T. (2005). Postnatal changes of vesicular glutamate transporter (VGluT)1 and VGluT2 immunoreactivities and their colocalization in the mouse forebrain. J. Comp. Neurol. 492, 263–288.

Narboux-Nême, N., Evrard, A., Ferezou, I., Erzurumlu, R.S., Kaeser, P.S., Lainé, J., Rossier, J., Ropert, N., Südhof, T.C., and Gaspar, P. (2012). Neurotransmitter release at the thalamocortical synapse instructs barrel formation but not axon patterning in the somatosensory cortex. J. Neurosci. 32, 6183–6196.

Nieto, M., Monuki, E.S., Tang, H., Imitola, J., Haubst, N., Khoury, S.J., Cunningham, J., Gotz, M., and Walsh, C.A. (2004). Expression of Cux-1 and Cux-2 in the subventricular zone and upper layers II-IV of the cerebral cortex. J. Comp. Neurol. 479, 168–180.

O'Leary, D.D. (1989). Do cortical areas emerge from a protocortex? Trends Neurosci. 12, 400–406.

O'Leary, D.D., and Sahara, S. (2008). Genetic regulation of arealization of the neocortex. Curr. Opin. Neurobiol. 18, 90–100.

Patra, R.C., Blue, M.E., Johnston, M.V., Bressler, J., and Wilson, M.A. (2004). Activity-dependent expression of Egr1 mRNA in somatosensory cortex of developing rats. J. Neurosci. Res. 78, 235–244.

Quairiaux, C., Armstrong-James, M., and Welker, E. (2007). Modified sensory processing in the barrel cortex of the adult mouse after chronic whisker stimulation. J. Neurophysiol. 97, 2130–2147.

Rakic, P., Ayoub, A.E., Breunig, J.J., and Dominguez, M.H. (2009). Decision by division: making cortical maps. Trends Neurosci. 32, 291–301.

Sato, H., Fukutani, Y., Yamamoto, Y., Tatara, E., Takemoto, M., Shimamura, K., and Yamamoto, N. (2012). Thalamus-derived molecules promote survival and dendritic growth of developing cortical neurons. J. Neurosci. 32, 15388–15402.

Schaeren-Wiemers, N., André, E., Kapfhammer, J.P., and Becker-André, M. (1997). The expression pattern of the orphan nuclear receptor RORbeta in

the developing and adult rat nervous system suggests a role in the processing of sensory information and in circadian rhythm. Eur. J. Neurosci. 9, 2687–2701.

Schlaggar, B.L., Fox, K., and O'Leary, D.D. (1993). Postsynaptic control of plasticity in developing somatosensory cortex. Nature 364, 623–626.

Simons, D.J., and Woolsey, T.A. (1984). Morphology of Golgi-Cox-impregnated barrel neurons in rat SmI cortex. J. Comp. Neurol. 230, 119–132.

Staiger, J.F., Flagmeyer, I., Schubert, D., Zilles, K., Kötter, R., and Luhmann, H.J. (2004). Functional diversity of layer IV spiny neurons in rat somatosensory cortex: quantitative morphology of electrophysiologically characterized and biocytin labeled cells. Cereb. Cortex 14, 690–701.

Sur, M., and Rubenstein, J.L. (2005). Patterning and plasticity of the cerebral cortex. Science 310, 805–810.

Toonen, R.F.G., and Verhage, M. (2007). Munc18-1 in secretion: lonely Munc joins SNARE team and takes control. Trends Neurosci. 30, 564–572.

Van der Loos, H., and Woolsey, T.A. (1973). Somatosensory cortex: structural alterations following early injury to sense organs. Science 179, 395–398.

Wang, Y., Yin, X., Rosen, G., Gabel, L., Guadiana, S.M., Sarkisian, M.R., Galaburda, A.M., and Loturco, J.J. (2011). Dcdc2 knockout mice display exacerbated developmental disruptions following knockdown of doublecortin. Neuroscience 190, 398–408.

Welker, E., and Van der Loos, H. (1986). Quantitative correlation between barrel-field size and the sensory innervation of the whiskerpad: a comparative study in six strains of mice bred for different patterns of mystacial vibrissae. J. Neurosci. 6, 3355–3373.

West, A.E., and Greenberg, M.E. (2011). Neuronal activity-regulated gene transcription in synapse development and cognitive function. Cold Spring Harb. Perspect. Biol. 3, a005744, http://dx.doi.org/10.1101/cshperspect.a005744.

Whitford, K.L., Dijkhuizen, P., Polleux, F., and Ghosh, A. (2002). Molecular control of cortical dendrite development. Annu. Rev. Neurosci. 25, 127–149.

Wijetunge, L.S., Till, S.M., Gillingwater, T.H., Ingham, C.A., and Kind, P.C. (2008). mGluR5 regulates glutamate-dependent development of the mouse somatosensory cortex. J. Neurosci. 28, 13028–13037.

Windrem, M.S., and Finlay, B.L. (1991). Thalamic ablations and neocortical development: alterations of cortical cytoarchitecture and cell number. Cereb. Cortex 1, 230–240.

Yoneshima, H., Yamasaki, S., Voelker, C.C.J., Molnár, Z., Christophe, E., Audinat, E., Takemoto, M., Nishiwaki, M., Tsuji, S., Fujita, I., and Yamamoto, N. (2006). Er81 is expressed in a subpopulation of layer 5 neurons in rodent and primate neocortices. Neuroscience 137, 401–412.

Zhou, L., Gall, D., Qu, Y., Prigogine, C., Cheron, G., Tissir, F., Schiffmann, S.N., and Goffinet, A.M. (2010). Maturation of "neocortex isole" in vivo in mice. J. Neurosci. 30, 7928–7939.

Zhuang, X., Masson, J., Gingrich, J.A., Rayport, S., and Hen, R. (2005). Targeted gene expression in dopamine and serotonin neurons of the mouse brain. J. Neurosci. Methods 143, 27–32.